

Differential Scanning Calorimetry

Authors

Benjamin Milkereit and Olaf Kessler
*Faculty of Mechanical Engineering
and Marine Technology*

Christoph Schick
Institute of Physics

University of Rostock
Germany

Determination of Critical Cooling Rate for Hardening Aluminum Alloys using HyperDSC

Abstract

When an aluminum alloy is solution annealed and afterwards cooled too slowly, an exothermal precipitation reaction occurs. With increasing cooling rate, the precipitation heat decreases. Since the precipitation reaction is relatively fast, a fast cooling rate on the differential scanning calorimeter (DSC) is essential to obtain the critical cooling rate which is the minimum cooling rate at which no precipitation heat is detectable. In this case, it was determined to be $375 (\pm 10)$ K/min. Such a fast cooling rate can be realized through PerkinElmer's HyperDSC® technology.

Introduction

For the strengthening of suitable aluminum alloys, a heat treatment known as age hardening is sometimes performed. Strength is thereby increased by the mechanism of particle strengthening. The particles, which cause the strengthening, have a typical size in the nanometer-scale. Age hardening contains three steps: solution annealing, quenching and aging. During solution annealing, the relevant alloying elements are dissolved in a solid solution. This state is frozen by quenching and a supersaturated solid solution (SSS) results. In a third step, the material is aged, naturally (at room temperature) or artificially (temperatures usually up to 200 °C), for a certain time to obtain a controlled precipitation of strengthening particles. The precipitation process follows an alloy-specific sequence. Maximum strength is reached when precipitate size and structure hinder dislocation movement most efficiently. These strengthening particles are very small compared to the incoherent equilibrium-phase particles.¹

When an age hardening aluminum alloy is solution annealed and afterwards cooled too slowly, a precipitation reaction occurs during cooling. This reaction must be eliminated completely to reach maximum strength during the following aging. Cooling must therefore be fast enough to suppress precipitation. On the other hand, cooling should be slow enough to avoid extensive residual stresses and distortions. In order to meet these conflicting requirements, cooling should be carried out just above the critical cooling rate, which is the slowest cooling rate where no precipitation reaction occurs. The influence of the cooling rate on the precipitation behavior is described by continuous cooling precipitation (CCP) diagrams. This information can be used to optimize the quenching step of the age-hardening process. Moreover, simulation of precipitation during the cooling step of the age-hardening process is impossible without CCP diagrams. However, for aluminum alloys, very few CCP diagrams exist because common procedures to record such diagrams for steels like dilatometry are not usable for aluminum alloys.

The precipitation reactions during cooling of the alloys are exothermic. Recently, it was reported that this precipitation reaction can be detected by differential scanning calorimetry (DSC) in a cooling-rate range from 5 to 475 K/min. It was found that with increasing cooling rate, the precipitation heat decreases. Consequently, the released heat has been established as a measure for the amount of precipitated particles.²⁻⁵

It is possible to record CCP diagrams with different methods in different ranges of cooling rates. Until now, no complete CCP diagrams for aluminum alloys have been published. In order to record complete CCP diagrams of aluminum alloys, the DSC method seems to be most informative because it supplies a measure for the amount of precipitates via the amount of released heat in dependence of cooling rate. However, the DSC studies cited cover only a narrow range of cooling rates. Nevertheless, scanning calorimetry is nowadays possible over a very wide range of cooling rates. Very slow scanning to follow near-equilibrium phase changes can be done, beside others, with heat-flux DSCs of the CALVET-type.⁶ Ultra-fast scanning calorimetry (up to 1 MK/s) is possible with thin-film-chip calorimeters.^{7,8} Such calorimeters are available. Nevertheless, they were not applied yet because they have to be adapted to the specific task. Furthermore, the DSC technique is an established method for the investigation of the precipitation sequence during reheating of samples, which are solution annealed and typically quenched in water.⁹⁻¹²

The purpose of this report is to present a method for recording full-range CCP diagrams for low to medium quench sensitive aluminum alloys in the range from very slow cooling near equilibrium (0.1 K/min) to some hundred K/min. The challenges here are relative high temperatures, a wide range of cooling rates and as the most difficult task, the detection of the disappearance of the precipitation reaction near the critical cooling rate. To detect the alloy-specific critical cooling rate, the DSC reaches its limits because of zero-released heat when the supersaturated solid solution is obtained completely. The challenge here is to distinguish objectively between a tiny reaction and instrumental noise. An additional problem is the deconvolution of overlapping reaction peaks. Despite the relative large samples, signal smearing is no problem due to the good thermal conductivity of aluminum. Compared to the research published so far in this field, the evaluation method is more objective. It also enables evaluation of the characteristic data in the case of overlapping reactions.

Materials and Methods

The presented investigation was performed with the age hardening aluminum-magnesium-silicon wrought alloy EN AW-6005A. This is an often-used alloy with medium alloying content. Therefore, a relatively low critical cooling rate was expected. Cylindrical samples were turned from an extruded profile. Samples were cylinders with sample masses from 32 mg to 1550 mg with dimensions from 4 to 6.5 mm in diameter and from 1 to 22 mm in length adapted to the cooling rate and calorimeter used. As an inert reference material for the DSC measurements EN AW-1050, pure aluminum with an Al-content of over 99.5 wt.-%, was used. The reference samples were turned out of a cast block. The detailed amounts of alloying elements of both materials are shown in Table 1.

Table 1. Alloying elements of investigated aluminum basis-material: EN AW-6005A and EN AW-1050 (inert reference material).

wt.-%	Si	Fe	Cu	Mn	Mg	Cr	Zn	Ti
EN AW-1050	0.09	0.32	0.002	0.004	0.001	0.001	0.01	0.004
EN AW-6005A	0.68	0.20	0.01	0.11	0.57	0.040	0.01	0.018

The samples were solution annealed and cooled in three different types of DSC devices. An EN AW-1050 reference sample was placed in the reference furnace. The cooling rate varies from very slow cooling (0.1 K/min – equilibrium is expected) in discrete intervals up to critical cooling rate whereby the precipitation is completely suppressed. Selected samples have been artificially aged afterwards. Following this, hardness testing and metallographic investigations have been performed to confirm the DSC results.

Some conditions were constant for all DSC experiments:

- Solution-annealing temperature and time were 540 °C, 20 min, respectively.
- Excess specific heat capacity was determined from all measurements. That means the difference in specific heat between alloy EN AW-6005A and EN AW-1050. Therefore, a baseline measurement was done for each cooling rate with EN AW-1050 samples in reference and sample furnaces.
- Measurements were done at ambient pressure.
- Artificial aging was done at 25 °C for 7 min followed by 180 °C for 4 h.

For each DSC device, different conditions have been identified to reach optimal results. The slowest experiments were done with a heat-flux DSC of CALVET-type (Setaram® DSC 121). Cooling rates in the intermediate range from 10 K/min to 30 K/min were performed employing the heat-flux type Mettler DSC 823. The fastest DSC used was a PerkinElmer® Pyris™ 1 DSC with HyperDSC® capabilities, which is a double-furnace power-controlled DSC. The samples were about 4 mm in diameter and 1 mm in height, which results in a sample mass of about 32 mg. The samples were placed on a plate of pure aluminum foil (5 mg) to prevent the micro furnace from element diffusion. An Intracooler 2P and pure nitrogen as purge gas were used. To reach maximum cooling rates, massive metal guard-ring inserts were attached (instead of the star-shaped guard-ring inserts). The block temperature is -80 °C. The DSC is covered by a glove box. This box was under slight over-pressure of dry air. Because of the dry conditions under the glove box, icing was reduced to a minimum. To avoid baseline drift problems, sample and baseline measurements were done one after the other.

HyperDSC is a DSC-analysis technique which delivers fast scanning rates. It requires a DSC instrument with an extremely fast response time and very high resolution and can only be achieved on a power-controlled DSC from PerkinElmer. In contrast to most heat-flux DSCs, a power-controlled DSC uses ultra-lightweight furnaces with very low thermal inertia and the fastest possible DSC response time. It allows very fast linear heat-up and cool-down scanning (up to 750 K/min) over a broad temperature range.

The curves were evaluated for the characteristic temperatures of the reaction: start- and end-temperature but also for peak area. The area under the peak(s) gives information about the released specific heat, which is called “specific precipitation heat”. This value is a measure for the amount of precipitates. In some experiments, at least two reactions overlap. The total precipitation heat measured is the sum of both released heats. For complete, continuous-cooling precipitation diagrams, a separation of each reaction is needed. Therefore, it was postulated that the single reaction causes a heat peak that is shaped like a Gaussian distribution curve. The measured curves were approximated as a sum of two Gaussian peaks (Figure 1).

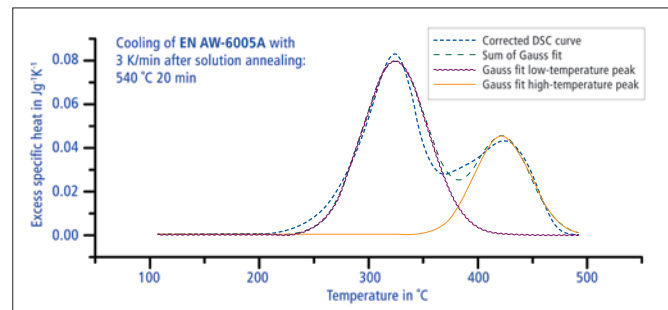


Figure 1. Evaluation: DSC curve fit with two Gaussian curves.

For the evaluation of start and end temperatures, defined points of the Gauss-curve were used:

$$C_p(T) = \left(\frac{\Delta H}{w \sqrt{\pi/2}} \right) e^{-2 \left(\frac{T - T_{peak}}{w} \right)^2}$$

$C_p(T)$ = excess specific heat

Fit parameters of Gauss-curve:

T_{peak} = peak-temperature

ΔH = peak-area

w = width of the Gauss-curve

Start and end temperatures were defined as $T_{\text{peak}} \pm w$. They correspond to the points where the peak deviates for about 15% of the peak height from the baseline. While these calculated start and end temperatures of the reaction are not the real reaction start and end temperatures, this method offers an objective evaluation of the characteristic temperatures also in the region of overlapping peaks.

The amount of released heat decreases with increasing cooling rate. One aim of this study is the detection of the critical cooling rate (CCR) at which the precipitation does not occur anymore. Therefore, an objective criterion is needed to determine when no precipitation heat is detectable in the measured curves. The challenge is to decide when a precipitation peak is above the noise level. The detection limit was defined by the following criteria:

- the reaction is detectable in at least three repeated experiments
- the reaction is detectable also at the next slower cooling rate
- specific precipitation heat is at least 0.1 J/g
- peak temperatures are in the same region as for the next slower rate

One example of a curve evaluation near the detection limit is shown in Figure 2. For correct curve interpretation, the evaluation must be done from slowest to faster cooling. Figure 3 gives an overview of all cooling rates and thereby information about the peak development.

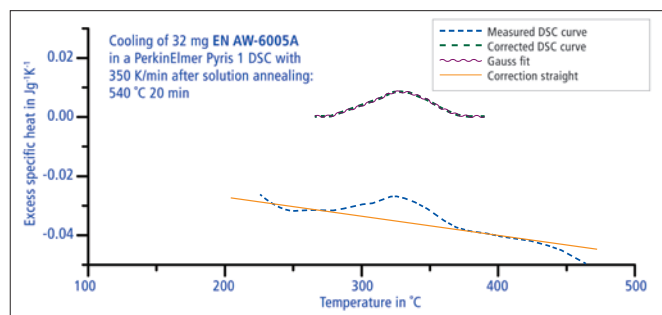


Figure 2. Curve evaluation near critical cooling rate. T_{Start} : 371 °C; T_{End} : 285 °C; specific precipitation heat: 0.44 J/g.

Results and Discussion

Figure 3 shows the bending-corrected excess-specific heat curves for the aluminum wrought alloy EN AW-6005A during cooling after solution annealing at 540 °C for 20 min.

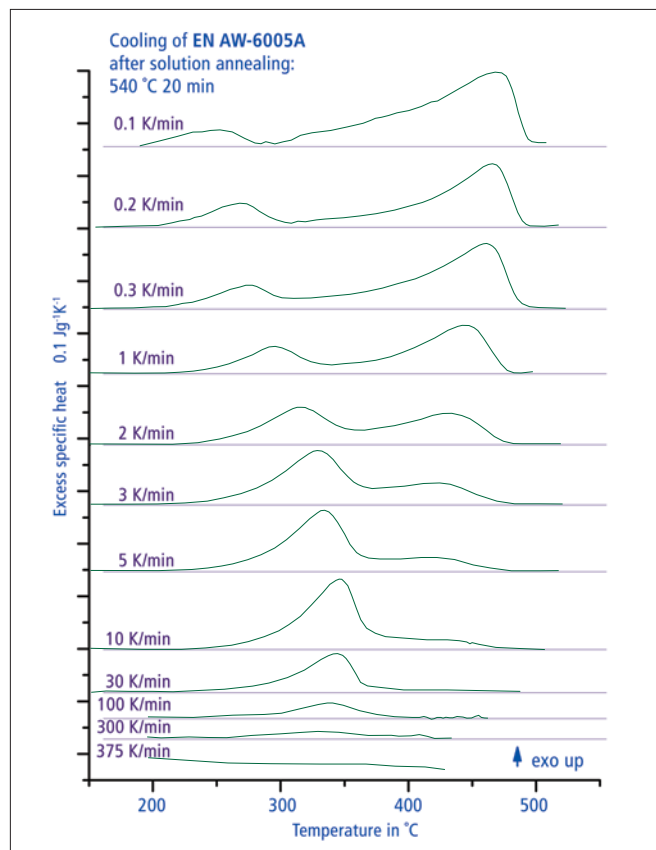


Figure 3. Overview of bending-corrected curves from three different types of DSC devices in a cooling-rate region from 0.1 to 375 K/min (0.1 to 5 K/min: Setaram 121; 10 to 30 K/min: Mettler 823; 100 to 375 K/min: PerkinElmer Pyris 1 DSC).

These curves were measured with three different types of DSC devices. The cooling rate ranges from close to equilibrium conditions at 0.1 K/min to critical cooling rate, which was identified at 375 K/min in this case. Figure 5 gives an overview of the peak-area and peak-temperature development. At the lowest cooling rate, near equilibrium, two main peaks were identified: a high-temperature peak with peak temperature of about 470 °C and a low-temperature peak with a peak temperature of about 250 °C. The range between the peak values is approximately 220 K. This precipitation temperature range shortens with increasing cooling rate. Near the critical cooling rate of the high-temperature peak (30 K/min), the difference between the peak values is only about 80 K (approximately 340 °C to 420 °C). This shows increasing

precipitation suppression with increasing cooling rate. At rates faster than 30 K/min, only the low-temperature peak occurs. At rates equal to or faster than 375 K/min, the precipitation is suppressed completely. The shift of the lower precipitation peak to higher temperatures with increasing cooling rate shows that thermal lag is not dominating the peak shifts observed.

Figure 4 presents the full-range continuous-cooling precipitation diagram of EN AW-6005A. This diagram displays the investigated cooling curves in a graph of temperature as a function of time. The time axis is scaled logarithmically. At 375 K/min (thick dotted line), there is no precipitation detectable any longer hence this was identified as the critical cooling rate for the aluminum wrought alloy EN AW-6005A. On the cooling curves of slower cooling, the start and end temperatures of the Gaussian peak-fit evaluation are inserted. In the range between 30 K/min down to about 1 K/min (cooling time from 540 °C to 50 °C: approximately 750 s to 20,000 s), two Gaussian peaks fit the measured curves reasonably well. In the range of even slower cooling, two Gaussian curves do not fit the measured curves well. The extreme slow curves show some indication of more than two reactions.

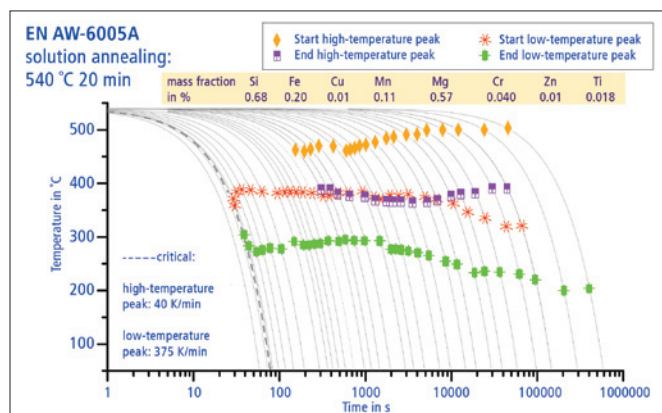


Figure 4. Full-range continuous-cooling precipitation diagram of EN AW-6005A. The solid lines correspond to linear cooling in the range between 500 K/min and 0.5 K/min.

It must be mentioned, that the CCP diagram is only valid for the investigated chemical composition, initial microstructure and solution-annealing conditions. The large range between high-temperature peak and low-temperature peak indicates probably more than two reactions or at least highly asymmetric peaks. The two-peak fit is still used because more peaks/reactions were not absolutely identifiable. In those cases with less correlation between the peak fit and the measured

curve, the peak fit is performed so that the sum of both peak areas agrees well with the integrated area of the measured curve. At the slowest cooling rate of 0.05 K/min, the lower limit of the DSCs used is reached. Because of the very small effects, the released heat due to the precipitation reaction is so small per time step that it is hardly detectable. Hence, the signal-to-noise ratio is poor.

The CCP diagram in Figure 4 delivers no information about the amount of released heat or the amount of precipitates respectively. This is shown in Figure 5, which displays the released specific precipitation heat and the Vickers-hardness after artificial aging as a function of cooling rate. The cooling-rate axis is scaled decreasing logarithmically. This is done to allow an easy comparison with the time scale of the CCP diagram.

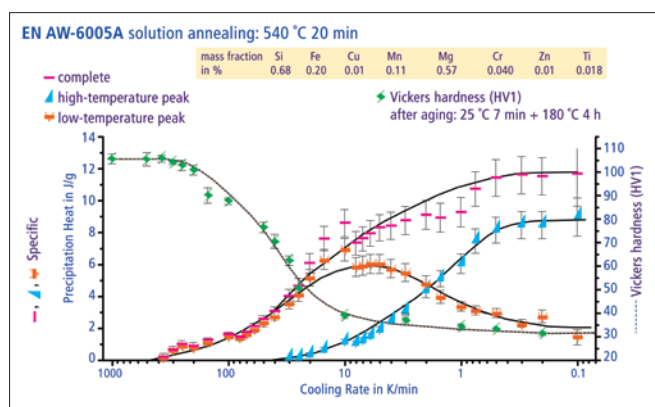


Figure 5. Specific precipitation heat and Vickers-hardness (HV-1) after aging as a function of the cooling rate. The displayed error bars show the uncertainty which results from evaluation.

From the peak-area determination, an uncertainty of about 10% is estimated. Additionally, the single areas of the double peak from the fits are displayed. There is a strong correlation between precipitation heat and hardness. If a precipitation occurs during cooling, it is hardly possible to strengthen the material during the following aging process. At the slowest cooling rate, the measured heat and the hardness approach their saturation. This fact indicates that the equilibrium state is approached.

Summary

For the aluminum-magnesium-silicon wrought alloy EN AW-6005A, age hardening was performed in three different types of differential scanning calorimeters (DSC), whereby the cooling rate varies over 3 orders of magnitude.

When an aluminum alloy is solution annealed and afterwards cooled too slowly, an exothermal precipitation reaction occurs. With increasing cooling rate, the precipitation heat decreases. The influence of the cooling rate on the precipitation behavior is described by continuous cooling precipitation (CCP) diagrams. With this information, the quenching step of the age-hardening process can be optimized. Furthermore, simulation of precipitation processes during the quenching step of the age hardening is impossible without the material data out of CCP diagrams.

Since the precipitation reaction is relatively fast, a fast cooling rate on the DSC is essential to obtain the critical cooling rate which is the minimum cooling rate at which no precipitation heat is detectable. In this case, it was determined to be 375 (± 10) K/min. Such a fast cooling rate can be realized on a PerkinElmer Pyris 1 DSC, which has double-furnace design and features HyperDSC fast-cooling capability. Without HyperDSC technology, it would be impossible to obtain the critical cooling rate and the complete CCP diagram of this aluminum alloy.

An extended version of this application note is available from *Thermochimica Acta* 492 (2009) 73-78.

References

1. I.J. Polmear, *Ligth alloys*, Butterworth-Heinemann, Oxford, 2006.
2. T. Herding, O. Kessler, F. Hoffmann, P. Mayr, An approach for Continuous Cooling Transformation (CCT) diagrams of aluminium alloys, *Aluminum Alloys 2002: Their Physical and Mechanical Properties* Pts 1-3 396-4 (2002) 869-874.
3. O. Kessler, R. von Bargaen, F. Hoffmann, H.W. Zoch, Continuous cooling transformation (CCT) Diagram of aluminium alloy Al-4.5Zn-1Mg, *Aluminium Alloys 2006*, Pts 1 and 2 519-521 (2006) 1467-1472.
4. B. Milkereit, O. Kessler, C. Schick, Continuous Cooling Precipitation Diagrams of Aluminium-Magnesium-Silicon Alloys, in: J. Hirsch, B. Skrotzki, G. Gottstein (Eds.), 11th International Conference on Aluminium Alloys, Deutsche Gesellschaft für Materialkunde e.V.; WILEY-VCH Weinheim, Aachen, Germany, 2008. pp. 1232-1237.
5. R. von Bargaen, Kontinuierliche Zeit- Temperatur-Ausscheidungsdiagramme der Aluminiumlegierungen 7020 und 7050, *Härtereitechnische Mitteilungen* 62(6) (2007).
6. E. Calvet, H. Prat, H. Skinner, *Recent progress in micro-calorimetry*, Pergamon Press, Oxford, London, New York, Paris, 1963.
7. S.A. Adamovsky, A.A. Minakov, C. Schick, Scanning micro-calorimetry at high cooling rate, *Thermochimica Acta* 403(1) (2003) 55-63.
8. A.A. Minakov, C. Schick, Ultrafast thermal processing and nanocalorimetry at heating and cooling rates up to 1 MK/s, *Review of Scientific Instruments* 78(7) (2007).
9. S. Esmaeili, X. Wang, D.J. Lloyd, W.J. Poole, On the precipitation-hardening behavior of the Al-Mg-Si-Cu, *Metall. Mater. Trans. A-Phys. Metall. Mater. Sci.* 34A(3) (2003) 751-763.
10. A. Gaber, A.M. Ali, K. Matsuda, T. Kawabata, T. Yamazaki, S. Ikeno, Study of the developed precipitates in Al-0.63Mg-0.37Si-0.5Cu (wt.%) alloy by using DSC and TEM techniques, *J. Alloy. Compd.* 432(1-2) (2007) 149-155.
11. M. Vedani, G. Angella, P. Bassani, D. Ripamonti, A. Tuissi, DSC analysis of strengthening precipitates in ultrafine Al-Mg-Si alloys, Springer, 2007. pp. 277-284.
12. X. Wang, S. Esmaeili, D.J. Lloyd, The sequence of precipitation in the Al-Mg-Si-Cu alloy AA6111, *Metall. Mater. Trans. A-Phys. Metall. Mater. Sci.* 37A(9) (2006) 2691-2699.